Low Mass Dileptons from Pb+Au Collisions at CERN SPS

Sourav Sarkar[1], Jan-e Alam[2] and T. Hatsuda[2]

[1] *Variable Energy Cyclotron Centre, 1/AF Bidhan Nagar, Calcutta 700 064 India*
[2] *Physics Department, University of Tokyo, Tokyo 113-0033, Japan*

Abstract

We show that the dilepton spectra measured by the CERES collaboration in Pb + Au interactions for various charge multiplicities can be reproduced by a hadronic initial state with reduction in the masses of the vector mesons in the thermal bath. Though such an effect may also be achieved by a large broadening of the spectral function we show that the photon spectra is insensitive to this. It is found that for higher multiplicities a good description of the data can also be obtained with quark gluon plasma initial state if the reduction of the vector meson masses in the mixed and hadronic phases is taken into account. We observe that a thermal source with initial temperature ~ 200 MeV can reproduce the observed enhancement in the low mass region of the dilepton spectra. It is not possible to state which one of the two initial states (QGP or hadronic) is compatible with the data. These findings are in agreement with our earlier results obtained from the analysis of the WA98 photon spectra. We estimate the number of $\pi - \pi$ collisions near the ρ-peak of the dilepton spectra and argue that thermal equilibrium may have been achieved in the system, justifying the use of hydrodynamical model to describe the space time evolution.

1 Introduction

One of the basic aims of research in highly relativistic nuclear collisions has been the creation and detection of Quark Gluon Plasma (QGP). Such an endeavour started at the BNL AGS, continued at the CERN SPS and is presently being pursued at the heavy ion experiments at the BNL RHIC. The principal motivation behind such a sustained and organized effort is that apart from being a confirmation of a long standing prediction of thermal QCD, the production of deconfined matter would actually recreate in the laboratory conditions which existed in the microsecond universe. A variety of signals of this exotic state of matter have been proposed and studied extensively over the last two decades. The suppression of the J/Ψ particle, the enhanced production of strange particles, specially strange antibaryons, excess production of photons and lepton pairs and the formation of disoriented chiral condensates are some of the well accepted probes of a deconfinement and/or a chiral symmetry restoring phase transition. In the recently concluded Pb run at the CERN SPS some of these, specially the magnitude of J/Ψ suppression has been claimed to be inexplicable in a non-QGP scenario [1].

Owing to their long mean free paths, electromagnetic signals *viz.* photons and dileptons are by far the most direct probes of the collision [2, 3, 4, 5, 6]. In fact they possess the unique property of being sufficiently less prone to secondary interactions because of their electromagnetic nature and yet are strong enough to be experimentally detectable. Moreover, unlike hadronic signals, photons and dileptons are produced all through the evolution process. In this connection one must

bear in mind that even if QGP is produced in the initial stages, the quarks and gluons will eventually form colour singlet hadrons before traveling to the detectors. Hence, in order to unmask the emissions from the QGP one must have a rather accurate estimation of the contributions from hadronic sources. In this aspect, the dilepton spectrum enjoys a clear advantage. This is because, though both photons and dileptons couple to hadrons through spin one ($J^P = 1^-$) mesons, the dilepton spectra exhibits a resonant structure which, in the low mass regime includes the ρ and the ω mesons. Now, it has been emphasized that the properties of the vector mesons undergo nontrivial medium modifications in a hot and/or dense medium such as likely to be produced in relativistic nuclear collisions. Consequently the spectral modifications of these vector mesons would be clearly revealed in the invariant mass spectra of the dileptons through the shift of the resonant peaks in the invariant mass spectra of dileptons.

Let us recall the various sources which produce dileptons in relativistic nuclear collisions. The principal source of thermal dileptons from the QGP and hadronic phases are the quark-antiquark and pion annihilation processes respectively. In the high mass region these compete with Drell-Yan pairs which are produced in primary interactions between incoming partons in the very early stages of the collision. The J/Ψ peak at 3 GeV marks the cut-off scale for thermal pairs from the plasma. Around this region the decays of D and B mesons also become an important source. The vector mesons which decay both during the expansion and after freeze-out can be identified easily from their characteristic peaks in the spectrum. Below the vector mesons, Dalitz decays of π^0, η, $\eta\prime$ and ω mesons provide the dominant source for dilepton production.

The observed enhancement of low-mass dileptons in Pb+Au collisions at the CERN SPS compared to the yield from hadronic decays at freeze-out as reported by the CERES Collaboration [7] has triggered a host of theoretical activity. Though the pion annihilation channel $\pi^+\pi^- \rightarrow l^+l^-$ accounts for a large fraction of this enhancement, it turns out that a quantitative explanation of the data requires the incorporation of medium modifications of the vector mesons. Li, Ko and Brown [8] were the first to achieve an agreement with the CERES data (for S+Au interactions) using a decreased ρ mass in the dense fireball. Rapp *et al* [9] have used a large broadening of the ρ meson spectral function due to scattering off baryons in order to explain the data. However, both approaches rely on a high baryon density for the dropping mass or the enlarged width of the ρ meson. Koch *et al* [10] finds very little effect due to baryons on the dilepton yield in the kinematic range of CERES experiment. It is worth emphasizing here that as yet it has not been possible to explain the observed low-mass enhancement of dileptons measured in the Pb+Au collisions [11] as well as in the S-Au [12] collisions at the CERN SPS in a scenario which does *not* incorporate in-medium effects on the vector meson mass. In short, the CERES dilepton data indicate a substantial change in the in-medium hadronic spectral function, either mass shift or broadening but fails to make any distinction between them.

We have shown earlier [13] that the WA98 photon spectra can be explained by either of the two scenarios of relativistic nuclear collision: (a) A +A →QGP→Mixed Phase→Hadronic Phase or (b) A + A →Hadronic Matter; with downward shift of

vector meson masses and initial temperature $\sim$ 200 MeV. The photon yield is insensitive to the broadening of vector mesons [14], although the CERES dilepton data admits such a scenario as mentioned above. In the present work we would like to see whether the CERES dilepton data can be described by the same scenarios (a and b) and with similar initial conditions which reproduce the WA98 photon spectra. The effects of the thermal shift of the hadronic spectral functions on both photon and dilepton emission have been considered in Ref. [14] for an exhaustive set of models. However, an appreciable change in the space-time integrated yield of electromagnetic probes was observed for universal scaling and Quantum Hadrodynamic (QHD) model. Therefore, in the present calculation we will consider these two cases.

The paper is organized as follows. In the following section we will briefly outline the phenomenology of medium effects on the vector mesons in the thermal environment which we have considered. In section 3 we will consider the static dilepton rates due to different processes. Then in section 4 we will describe the dynamics of space-time evolution followed by the results of our calculation in section 5. We will conclude with a summary and discussions in section 6.

2 Medium Effects

A substantial amount of literature has been devoted to the issue of temperature and/or density dependence of hadrons within various models (see [14, 15, 16, 17, 18] for a review). In Ref. [14] we have discussed the effects of spectral changes of hadrons on the electromagnetic probes in detail. In this work we will consider medium modifications of vector mesons in two different scenarios where non-trivial effects on the dilepton spectra were seen. These are: the universal scaling hypothesis and the Quantum Hadrodynamic (QHD) model.

In the scaling hypothesis, the parametrization of in-medium quantities (denoted by $*$) at finite T is

$$\frac{m_V^*}{m_V} = \frac{f_V^*}{f_V} = \frac{\omega_0^*}{\omega_0} = \left(1 - \frac{T^2}{T_c^2}\right)^{\lambda}, \tag{1}$$

where V stands for vector mesons, f_V is the coupling between the electromagnetic current and the vector meson field and ω_0 is the continuum threshold. Mass of the nucleon also varies with temperature according to Eq. (1) (pseudo scalar masses remain unchanged). The particular exponent $\lambda = 1/2$ (1/6) is known as Nambu (Brown-Rho) scaling. We will use $\lambda = 1/2$ in our calculations. Note that there is no definite reason to believe that all the in-medium dynamical quantities are dictated by a single exponent λ. This is the simplest possible ansatz (see [14] for a discussion). The effective mass of a_1 is estimated by using Weinberg's sum rules [19].

In the Quantum Hadrodynamic model [20, 21] of nuclear matter the vector meson properties are modified due to coupling with nucleonic excitations. The nucleons interact through the exchange of scalar σ and the vector ω mesons and their mass is modified due to the scalar condensate. This is evaluated in the Relativistic Hartree Approximation (RHA). Coupling with these modified nucleonic excitations induce changes in the ρ and ω meson masses. This modification is contained in the

meson self energy which appears in the Dyson-Schwinger equation for the effective propagator in the medium. The interaction vertices are provided by the Lagrangian

$$\mathcal{L}^{\rm int}_{VNN} = g_{VNN}\left(\bar{N}\gamma_\mu\tau^a N V^\mu_a - \frac{\kappa_V}{2M_N}\bar{N}\sigma_{\mu\nu}\tau^a N\partial^\nu V^\mu_a\right), \tag{2}$$

where $V^\mu_a = \{\omega^\mu, \vec{\rho}^\mu\}$, M_N is the free nucleon mass, N is the nucleon field and $\tau_a = \{1, \vec{\tau}\}$, $\vec{\tau}$ being the Pauli matrices. The real part of the vector meson self-energy due to $N\bar{N}$ polarization is responsible for the mass shift. The details of the calculations can be found in our previous work [22, 23] (see also [24]) and we do not reproduce them here. The masses of the ρ and ω are parametrized as a function of T as

$$\begin{aligned} m^*_\rho &= m_\rho\left[1 - 0.127\left(\frac{T(\text{GeV})}{0.16}\right)^{5.24}\right] \\ m^*_\omega &= m_\omega\left[1 - 0.0438\left(\frac{T(\text{GeV})}{0.16}\right)^{7.09}\right]. \end{aligned} \tag{3}$$

It is important to note that unlike the universal scaling the ρ and ω masses decrease differently with temperature due to different coupling strength with nucleons (Eq.(2)).

3 Dilepton Emission Rate

In this section, we briefly recapitulate the main equations relevant for evaluating dilepton emissions from a thermal source. The emission rate of dileptons with four momentum q_μ can be expressed in terms of the imaginary part of the retarded current-current correlation function as

$$\frac{dR}{d^4q} = \frac{\alpha}{12\pi^4\, q^2}\text{Im}W^R_{\mu\mu}\, f_{BE}(q_0) \tag{4}$$

where the electron mass has been taken to be zero. Putting $d^4q = \pi\, dM^2\, p_T dp_T\, dy$, where M, p_T and y are the invariant mass, transverse momentum and rapidity of the lepton pair respectively, this is written as

$$\frac{dR}{dM^2\, p_T\, dp_T\, dy} = \frac{\alpha}{12\pi^3}\frac{1}{M^2}\, e^{-M_T\cosh y/T}\ \text{Im}W^R_{\mu\mu}. \tag{5}$$

in the Boltzmann approximation.

The information about the specific processes occurring in the thermal medium which produces the dileptons resides in the current correlator $W^{\mu\nu}$. In the QGP, the dominant channel for dileptons production is quark-antiquark annihilation. The rate for this process is obtained from the lowest order diagram contributing to the current correlator $W^{\mu\nu}$. In the limit of vanishing quark masses, the rate for the process $q\bar{q} \to e^+e^-$ is obtained as,

$$\frac{dR}{dM^2\, p_T\, dp_T\, dy} = \frac{5}{9}\,\frac{\alpha^2}{4\pi^3}\, e^{-M_T\cosh y/T}. \tag{6}$$

Now let us consider dilepton production in the hadronic medium. The process $\pi^+\pi^- \rightarrow e^+e^-$ is known to be the most dominant source of dilepton production from hadronic matter. It was shown earlier that the width of the ω meson can be large due to various reactions occurring in the thermal bath. The most dominant process, among others, is $\omega\pi \rightarrow \pi\pi$ [25]. In view of this we also take into account the in-medium decay $\omega \rightarrow e^+e^-$ as well as $\rho \rightarrow e^+e^-$. In order to obtain the rate from Eq. (5) the electromagnetic current correlator is expressed in terms of the effective propagator of the vector particle in the thermal medium using vector meson dominance (VMD) to obtain

$$\mathrm{Im}W^R_{\mu\mu} = \frac{3e^2 m^{*4}_\rho}{g^2_{\rho\pi\pi}} \left[\frac{\mathrm{Im}\Pi^{\rho R}}{(M^2 - m^{*2}_\rho) + [\mathrm{Im}\Pi^{\rho R}]^2}\right]. \tag{7}$$

where $\Pi^{\rho R}$ is the self energy of the ρ arising out of interaction with excitations in the medium. For a ρ meson propagating with energy q_0 and three momentum $\vec{q}$ the ρ width is given by

$$\begin{aligned}\Gamma_{\rho\rightarrow\pi\,\pi}(q_0,\vec{q}) &= \frac{g^2_{\rho\pi\pi}}{48\pi}\,W^3(s)\,\frac{s}{q_0}\,\left[1+\frac{2T}{W(s)\sqrt{q_0^2-s}}\right. \\ &\left.\times\ln\left\{\frac{1-\exp[-\frac{\beta}{2}(q_0+W(s)\sqrt{q_0^2-s})]}{1-\exp[-\frac{\beta}{2}(q_0-W(s)\sqrt{q_0^2-s})]}\right\}\right]\end{aligned} \tag{8}$$

where $s = M^2 = q_0^2 - \vec{q}^2$ and $W(s) = \sqrt{1-4m_\pi^2/s}$.

In a thermal medium the production of an off-shell vector meson (V) of four momentum q (where $q^2 = M^2$) and its subsequent decay into a lepton pair leads to the dilepton emission rate [26]

$$\frac{dR}{d^4q} = 2\frac{(2J+1)}{(2\pi)^3}\,f_{BE}\,M\Gamma^{\rm vac}_{V\rightarrow l^+l^-}\,\left[\frac{1}{\pi}\frac{\mathrm{Im}\Pi^R_V}{(q^2-m_V^2+\mathrm{Re}\Pi^R_V)^2+(\mathrm{Im}\Pi^R_V)^2}\right]. \tag{9}$$

As before this reduces to

$$\frac{dR}{dM^2\,p_T\,dp_T\,dy} = \frac{3}{4\pi^3}\Gamma^{\rm vac}_{V\rightarrow l^+l^-}\frac{M^2\,\Gamma_\rho(M)}{(M^2-m^{*2}_\rho)^2+M^2\Gamma^2_\rho(M)}\,e^{-M_T\cosh y/T} \tag{10}$$

with the vacuum decay width given by

$$\Gamma^{\rm vac}_{V\rightarrow l^+\,l^-} = \frac{4\pi\alpha}{3M}g^2_{V\gamma}. \tag{11}$$

The coupling $g_{V\gamma}$ can be determined by using vector meson dominance and the observed decay width of $V \rightarrow e^+e^-$ in vacuum.

4 Space-Time Evolution

The observed spectrum originating from an expanding hadronic matter is obtained by convoluting the static rates given above with the expansion dynamics. The

usual space-time picture of the evolution is as follows. Matter initially formed as a hot hadronic gas expands and cools till freeze-out. However, in a phase transition scenario, matter produced as QGP expands and cools to the phase transition temperature T_c. A mixed phase of coexisting quark and hadronic matter follows. After all the quark matter has converted to hadrons, the hot hadron matter expands and cools till freeze-out. In this work we use Bjorken-like [27] hydrodynamical model for the isentropic expansion of the matter. The essential input at this stage is the equation of state (EOS) which provides the cooling law. For the QGP sector we use the bag model equation of state with two flavour degrees of freedom. The temperature in the QGP phase evolves according to Bjorken scaling law $T^3\,\tau = T_i^3\tau_i$.

The hadronic phase is taken to consist of π, ρ, ω, η and a_1 mesons and nucleons. The energy density and pressure for such a system is given by,

$$\epsilon_H = \sum_{i=mesons} \frac{g_i}{(2\pi)^3}\int d^3p\, E_i\, f_{BE}(E_i,T) + \frac{g_N}{(2\pi)^3}\int d^3p\, E_N\, f_{FD}(E_N,T) \qquad (12)$$

and

$$P_H = \sum_{i=mesons} \frac{g_i}{(2\pi)^3}\int d^3p \frac{p^2}{3\,E_i} f_{BE}(E_i,T) + \frac{g_N}{(2\pi)^3}\int d^3p \frac{p^2}{3\,E_N} f_{FD}(E_N,T) \qquad (13)$$

where the sum is over all the mesons under consideration and N stands for nucleons and $E_i = \sqrt{p^2+m_i^2}$. The entropy density is parametrized as,

$$s_H = \frac{\epsilon_H + P_H}{T} \;\equiv\; 4a_{\rm eff}(T)\,T^3 = 4\frac{\pi^2}{90} g_{\rm eff}(m^*(T),T)T^3 \qquad (14)$$

where $g_{\rm eff}$ is the effective statistical degeneracy. Thus, we can visualize the finite mass of the hadrons having an effective degeneracy $g_{\rm eff}(m^*(T),T)$. (For a possible parametrization of entropy density consistent with lattice QCD we refer to [28]). The variation of temperature from its initial value T_i to final value T_f (freeze-out temperature) with proper time (τ) is governed by the entropy conservation

$$s(T)\tau = s(T_i)\tau_i \qquad (15)$$

In the present scenario the velocity of sound, c_s becomes a function of T,

$$c_s^{-2} = \frac{T}{s_H}\frac{ds_H}{dT} = \left[\frac{T}{g_{\rm eff}}\frac{dg_{\rm eff}}{dT} + 3\right] \qquad (16)$$

We will see later that c_s differs substantially from its value corresponding to an ideal gas.

The initial temperature of the system is obtained by solving the following equation

$$\frac{dN_\pi}{dy} = \frac{45\zeta(3)}{2\pi^4}\pi\, R_A^2 4a_{\rm eff}T_i^3\tau_i \qquad (17)$$

where dN_π/dy is the total pion multiplicity ($\sim 1.5\times$ charge multiplicity), R_A is the radius of the system, τ_i is the initial thermalization time and $a_{\rm eff} = (\pi^2/90)\,g_{\rm eff}(T_i)$. When the system is produced in the QGP phase, $g_{\rm eff}$ in the above equation is replaced by g_{QGP} which for two quark flavours is 37. If the quark and gluon masses

are non-zero in the thermal bath then the effective degeneracy of the QGP, $g^{\rm eff}_{\rm QGP}$, defined by Eq. (14) can be lower than 37, resulting in a higher value of T_i for a given multiplicity according to Eq. (17). Note that the change in the expansion dynamics as well as the value of the initial temperature due to medium effects relevant for a hot hadronic gas also enters through the effective statistical degeneracy.

5 Results

We will now compare our results with experimental spectra obtained by the CERES collaboration in Pb+Au collisions at the CERN SPS. In the central rapidity region the entropy per baryon is found to be quite large $\sim 40 - 50$ [29, 30]. Thus the finite baryon density effects are neglected here. The dilepton spectra for various charge multiplicities are evaluated both with and without a phase transition. In all the cases we will assume an initial formation time $\tau_i = 1$ fm/c and freeze-out temperature, $T_f = 120$ MeV [31]. The initial temperatures depend on the scenario concerned. They are listed below in Table 1. The second column gives the initial temperatures in a phase transition scenario with QGP as the initial state. The next two columns are the values corresponding to a hot hadronic gas scenario with vacuum and QHD masses respectively. When mass modifications are incorporated using universal scaling the initial state depends on the particular value of T_c that one considers. In view of the prevailing uncertainties in its value we have considered T_c =170, 190 and 200 MeV [32]. For $dN_{ch}/d\eta$ = 150 and 210, $T_i \leq 170$ MeV. Therefore, for these cases we consider the hadronic initial states only. However, for events with $dN_{ch}/d\eta$=270 and 350 the initial temperature can be larger than the critical temperature as seen below.

	QGP	vacuum mass	QHD	Scaling T_c=170 MeV	Scaling T_c=200 MeV
$dN_{ch}/d\eta$	T_i (MeV)	T_i (MeV)	T_i (MeV)	T_i (MeV)	T_i (MeV)
150	161	209	199	168	181
210	171	219	206	171	187
270	179	227	212	179	192
350	187	235	217	187	196

Table 1 : Values of initial temperature obtained by solving Eqs. 14 and 17 self-consistently for various values of $dN_{ch}/d\eta$.

The velocity of sound, which governs the space-time evolution of the system, is obtained by solving Eqs. (14) and (16) self consistently. This is shown in Fig. 1 where hadronic masses vary as a function of temperature according to universal scaling and QHD model. It is noted that the value of c_s^2 in the hadronic phase is less than that of a massless ideal gas ($c_s^{ideal} = 1/\sqrt{3}$) indicating substantial interaction among the various constituents of the system. This is consistent with the results of Ref. [28].

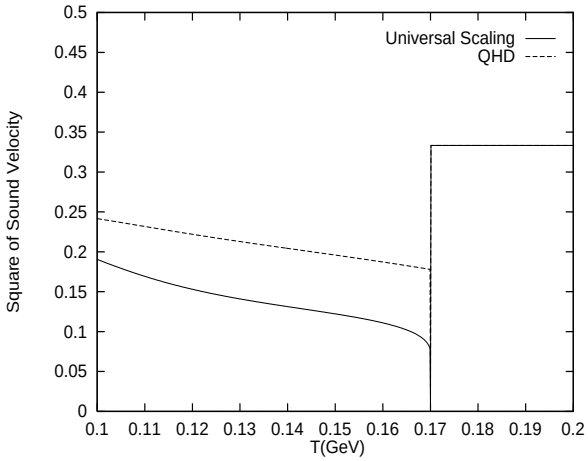

Figure 1: Velocity of sound as a function of temperature, for different mass variation scenario for the hadrons in a deconfinement phase transition scenario.

We have considered dileptons with transverse momentum p_T above 200 MeV/c and an opening angle $\Theta_{ee} > 35$ mrad. These are kinematical cuts relevant for the CERES detector and are incorporated as described in the appendix of Ref. [12]. In all the figures, the quantity $\langle N_{ch} \rangle$ indicates the average number of charged particles per unit rapidity interval in the pseudorapidity range $2.1 < \eta < 2.65$. In all the cases background due to hadron decays are added to the thermal yields.

In Figs. 2 and 3 we have shown the invariant mass spectra of dileptons corresponding to $\langle N_{ch} \rangle$=150 and 210 respectively. In these cases the initial temperature is not high enough to favour a phase transition to QGP. Hence we have considered a hot hadronic gas as the initial state. The medium effects are considered according to universal scaling (Eq. (1) with $\lambda = 1/2$) and the QHD model. For $dN_{ch}/d\eta = 150$ a good description of the data is realized with $T_i = 168$ MeV obtained by solving Eq. (17) for the mass variation given in Eq. (1) with $\lambda = 1/2$ (dashed line). For QHD however, $T_i = 199$ MeV (because of lower $g_{\rm eff}$) resulting in a larger dilepton yield. The theoretical yield (dash-dotted line) overestimate the data in the region of ρ-peak because of smaller reduction in ρ-mass in QHD. For $dN_{ch}/d\eta = 210$ the initial temperatures are $T_i = 171$ and 206 MeV for universal scaling and QHD model respectively. The dilepton yield is well reproduced for both the cases. Considering the experimental error bars it is not possible to state which one of the two is compatible with the data.

In Fig. 4 we display the results for $dN_{ch}/d\eta = 270$. In this case apart from the hadronic gas scenario we have also considered a deconfined initial state with $T_i = 179$ MeV which evolves into a hadronic gas via a mixed phase. The observed enhancement of the dilepton yield around $M \sim 0.3-0.6$ GeV can be reproduced with the QGP initial state, once the variation of vector meson masses in the mixed and the hadronic phases are taken into account (solid line). The data is also reproduced by a hadronic initial state with $T_i = 212$ and 192 MeV for QHD (dashed) and universal mass variation scenario (dash-dotted) respectively. The ρ-peak in the dilepton spectra shifts towards lower M for universal scaling compared to QHD model, indicating a strong medium effect in the former case. In this case again

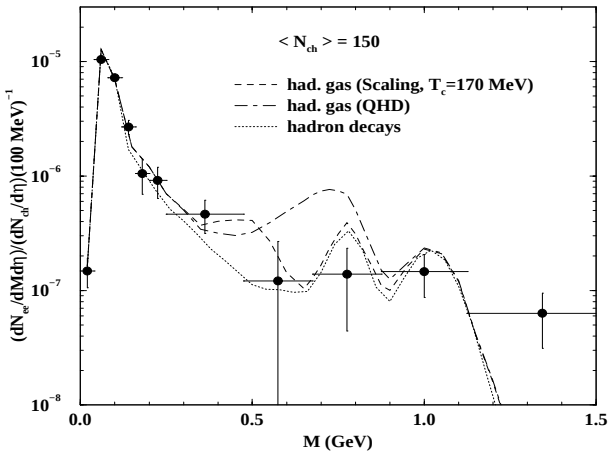

Figure 2: Dilepton spectra for $\langle N_{ch}\rangle$=150. The dashed line (dash-dotted) indicates e^+e^- pair yield when the system is formed in the hadronic phase and hadronic masses vary according to universal scaling (QHD). Note that these also include the yield from hadronic decays at freezeout (dotted line).

it is impossible to differentiate between the QHD model and the universal scaling scenario.

Finally, in Fig. 5 we depict the dilepton spectra for QGP and hadronic initial states for $dN_{ch}/d\eta = 350$. Results with hadronic initial state and universal scaling of hadronic masses with temperature seem to describe the data reasonably well. However, if we consider the temperature dependent mass from QHD (dotted line) then the low M enhancement of the experimental yield is not reproduced. For $T_i = 187$ MeV (see table 1) with a QGP initial state it is not possible to explain the measured dilepton spectra (result not shown in the figure). However, as we mentioned in section 4, the value of T_i in the 2-flavour QGP may be larger if g_{QGP} is lower than 37 due to interactions among quarks and gluons (leading to non-zero masses of quarks and gluons) in the QGP phase. A good description of the data can be obtained by taking $T_i = 200$ MeV for the QGP initial state both for $T_c = 170$ (solid) and 190 (dashed) MeV. All these results seem to indicate an initial temperature $\sim$ 200 MeV, a value which we obtained earlier by analyzing WA98 photon data.

In Fig. 6 we demonstrate the effects of a large broadening of the vector meson spectral function on the photon spectra. To estimate the photon yield from hadronic matter, we have considered the reactions [33], $\pi\,\rho \rightarrow \pi\,\gamma$, $\pi\,\pi \rightarrow \rho\,\gamma$, $\pi\,\pi \rightarrow \eta\,\gamma$, $\pi\,\eta \rightarrow \pi\,\gamma$ and the decays $\rho \rightarrow \pi\,\pi\,\gamma$ and $\omega \rightarrow \pi\,\gamma$. The invariant amplitudes for all these processes can be found in Refs. [22, 23]. We have also considered photon emission due to the reaction $\pi\,\rho \rightarrow a_1 \rightarrow \pi\,\gamma$ [14]. The width of ρ has been taken as 1 GeV, independent of temperature purely for the purpose of demonstration. In a thermal medium, even if a huge enhancement of the width takes place as a result of interactions, near the freeze-out temperature the vector meson will regain its vacuum properties. So, by taking a large constant width throughout the evolution process we have overestimated its effect on the photon spectra. However, it is clear from Fig. 6, the effect is still small; the experimental photon data with the

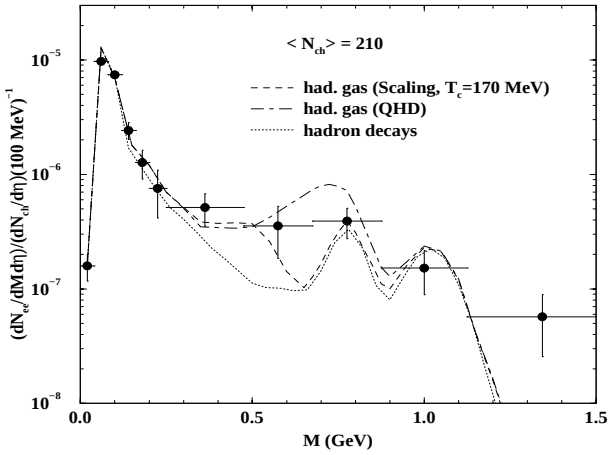

Figure 3: Same as Fig. 2 for $\langle N_{ch}\rangle$=210.

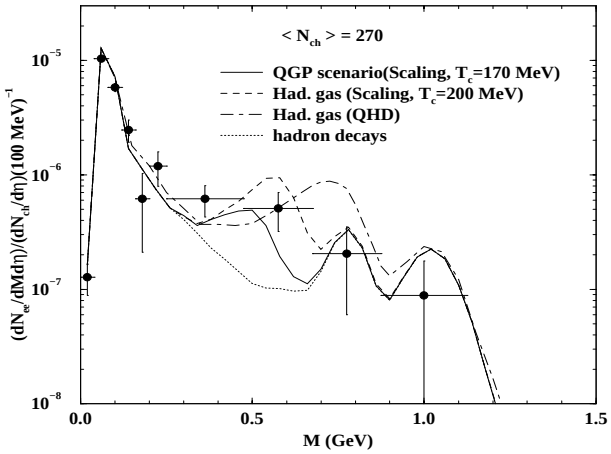

Figure 4: Dilepton spectra for $\langle N_{ch}\rangle$=270 for different initial states and mass variation scenarios. Solid line indicates dilepton yield when QGP is formed. (Here QGP scenario indicates sum of yields from QGP phase+QGP part of the mixed phase +hadronic part of the mixed phase +hadronic phase) The dashed line (dash-dotted) indicates e^+e^- pair yield when the system is formed in the hadronic phase and vector meson masses vary according to universal scaling (QHD).

current statistics can not detect such effects. We do not show the effects of large ρ broadening on the dilepton spectra in this work as there exists a comprehensive review on this subject [17].

Throughout this work we have assumed thermal equilibrium of the system. How good is this assumption? We recall that the number of $\pi - \pi$ collisions, $N_{\pi\pi}$ in the region $M \sim m_\rho^*$ can be estimated from the following equation [34]:

$$N_{\pi\pi} = 2 \times 3 \times \frac{\Gamma_\rho^*}{B_\rho} \frac{dN}{dM d\eta}|_{M=m_\rho^*} \tag{18}$$

where B_ρ is the branching ratio for the decay $\rho \rightarrow e^+e^-$. The factor 3 comes from the isospin combinations and counting collisions per particle gives a further factor of 2. The number of collisions, $N_{\pi\pi}$ is estimated as 200, 254, 1050 and 1875 for $dN_{ch}/d\eta$=150, 210, 270 and 350 respectively for the universal mass variation scenario (which describe the data well for all multiplicities). We assume that thermal equilibrium may be realized in the system if $N_{\pi\pi} \geq 1$ (a similar argument was put forward in ref. [35] regarding the equilibration of gluons). Considering the total multiplicity $= 1.5 \times dN_{ch}/d\eta$, we point out that thermal equilibrium may not be realized in the case of $dN_{ch}/d\eta = 150$ and 210 since the number of collisions per particle in the system, $\sim N_{\pi\pi}/(1.5 dN_{ch}/d\eta) < 1$. Interestingly, we note that for $dN_{ch}/d\eta = 150$ the thermal source is not required to describe the data; the yield from hadron decays explain the data well. For $dN_{ch}/d\eta = 210$, however, the yield from hadronic decays underestimate the data. For higher multiplicities ($dN_{ch}/d\eta = 270$ and 350) the number of collisions per particle ≥ 3, indicating that thermal equilibrium may have been achieved, justifying the use of hydrodynamics to describe the space time evolution of the system. We have also checked that the condition, $\tau^\pi_{\rm scatt} < \tau_{\rm exp}$ is satisfied throughout the evolution process, indicating that the use of hydrodynamics is reasonable for space-time description [36]. Here $\tau^j_{\rm scatt} = (\sum_i \langle v_{ij} \rangle \sigma_{ij} n_j)^{-1}$, is the mean collision time, v_{ij} is the relative velocity, σ_{ij} is the scattering cross section, n_j is the particle density of specie j and $\tau_{\rm exp} = \tau_i (T_i/T)^{1/c_s^2}$ is the expansion time scale.

It was proposed earlier [37] that the onset of deconfinement can be inferred through the dilepton yield if the quantity, $dN_{ee}/d\eta/(dN_{ch}/d\eta)^2$ (a quantity which is free from uncertainties in initial conditions) reaches a plateau with increasing $dN_{ch}/d\eta$ and the height of the plateau will be a measure of T_c. We evaluated the above quantity for the four charge multiplicities mentioned above and did not observe any plateau.

6 Summary and Discussions

We have studied the dilepton yield measured by CERES experiment for various values of charge multiplicities in Pb + Au interactions. It is observed that for lower multiplicities ($dN_{ch}/d\eta = 150$ and 210), dileptons seem to originate from a hadronic source with initial temperature ~ 170 MeV. For the higher values of the charge multiplicity (270 and 350), however, the data can be described by both QGP and hadronic initial states. The value of the initial temperature realized in the high multiplicity events is similar to that obtained from the analysis of WA98 photon

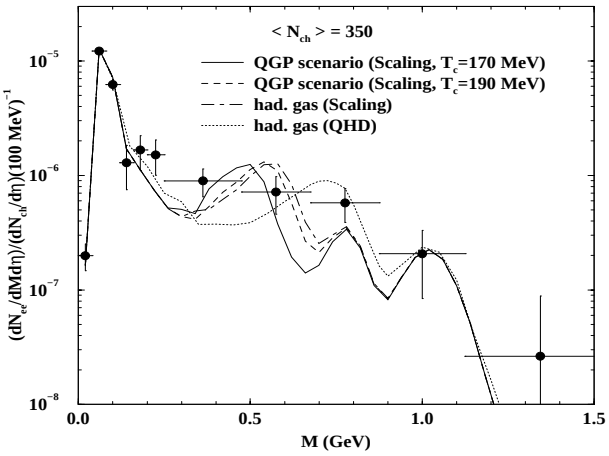

Figure 5: Dilepton spectra for $\langle N_{ch} \rangle$=350 for different initial states and mass variation scenarios. Solid (dashed) line indicates dilepton yield when QGP is formed with $T_i = 200$ MeV and $T_c = 170$ MeV (190 MeV). The dash-dotted (dotted) line indicates e^+e^- pair yield when the system is formed in the hadronic phase and vector meson masses vary according to universal scaling (QHD).

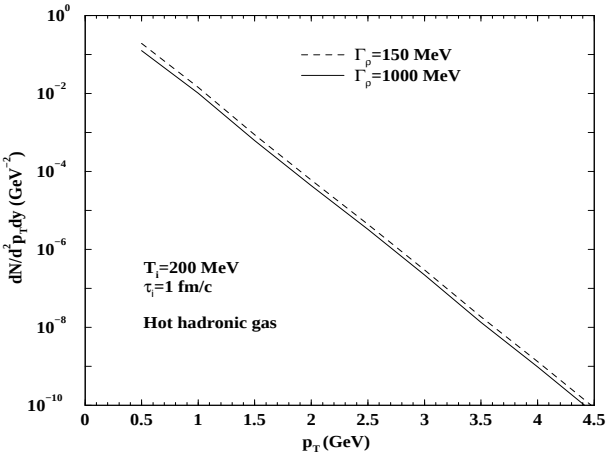

Figure 6: Thermal photon spectra for $T_i = 200$ MeV and $\tau_i = 1$ fm/c. Solid (dashed) line indicates photon yield with large broadening of the ρ spectral function (vacuum spectral function).

spectra. We find that both the enhancement in the photon and dilepton yields measured by WA98 and CERES collaborations respectively are due to a thermal source with initial temperature ~ 200 MeV. However, it is difficult to state which one of the two phases, QGP or hadronic gas is realized in the initial state of matter produced after the collision. We also point out that the number of $\pi - \pi$ collisions extracted from the dilepton spectra near m_ρ are reasonably high in order to maintain thermal equilibrium in the system. We conclude by noting that to reproduce the data for large charge multiplicities either a large broadening of ρ or a substantial reduction in vector meson masses is required. Though it is difficult to draw a firm conclusion at this point, these phenomena are closely related to deconfinement or chiral symmetry restoring transition. Indeed, in Ref. [38] it has been shown that a parametrization which mimics the dilepton emission rate from $q\bar{q}$ annihilation reproduce the CERES Pb+Au data well. At this critical and interesting juncture we look forward to the experiments at RHIC where larger and hotter systems are likely to be produced. Along with quantitative gains in all the signals there is a distinct possibility of electromagnetic radiation from the QGP phase which will pave the way for an unambiguous conclusion regarding the formation of this novel form of matter.

Acknowledgement: We are grateful to B. Lenkeit and J. Stachel for providing us with the experimental data. We also thank Bikash Sinha and Tapan K. Nayak for very fruitful discussions. J.A. is grateful to the Japan Society for Promotion of Science (JSPS) for financial support. J.A. and T.H. are also supported by Grant-in-aid for Scientific Research No. 98360 of JSPS.

References

[1] See *e.g.* Proc. of Quark Matter'99, Nucl. Phys. **A 661** (1999).

[2] L. McLerran and T. Toimela, Phys. Rev. **D 31**, 545 (1985).

[3] C. Gale and J. I. Kapusta, Nucl. Phys. **B357**, 65 (1991).

[4] E. V. Shuryak, Phys. Rep. **61**, 71 (1980).

[5] J. Alam, S. Raha and B. Sinha, Phys. Rep. **273**, 243 (1996).

[6] W. Cassing and E. L. Bratkovskaya, Phys. Rep., **308**, 65 (1999).

[7] G. Agakichiev *et al*, CERES Collaboration, Phys. Lett. **B 422**, 405 (1998), B. Lenkeit, Doctoral Thesis, Universitaet Heidelberg (1998).

[8] G. Q. Li, C. M. Ko and G. E. Brown, Phys. Rev. Lett. **75**, 4007 (1995).

[9] R. Rapp, G. Chanfray and J. Wambach, Phys. Rev. Lett. **76**, 368 (1996).

[10] V. Koch, nucl-th/9903008; V. Koch and C. Song, Phys. Rev. **C54**, 1903 (1996).

[11] C. M. Hung and E. V. Shuryak, Phys. Rev. **C56**, 453 (1997).

[12] J. Sollfrank, P. Huovinen, M. Kataja, P. V. Ruuskanen, M. Prakash and R. Venugopalan, Phys. Rev. **C55**, 392 (1997).

[13] J. Alam, S. Sarkar, T. Hatsuda, T. K. Nayak and B. Sinha, hep-ph/0008074.

[14] J. Alam, S. Sarkar, P. Roy, T. Hatsuda and B. Sinha, Ann. Phys.(in press), hep-ph/9909267.

[15] T. Hatsuda and T. Kunihiro, Phys. Rep. **247**, 221 (1994).

[16] G. E. Brown and M. Rho, Phys. Rep. **269**, 333 (1996).

[17] R. Rapp and J. Wambach, hep-ph/9909229.

[18] R. D. Pisarski, hep-ph/9503330.

[19] S. Weinberg, Phys. Rev. Lett. **18**, 507 (1967).

[20] B. D. Serot and J. D. Walecka, *Advances in Nuclear Physics Vol. 16*, Plenum Press, New York 1986.

[21] S. A. Chin, Ann. Phys. **108**, 301 (1977).

[22] S. Sarkar, J. Alam, P. Roy, A. K. Dutt-Mazumder, B. Dutta-Roy and B. Sinha, Nucl. Phys. **A634**, 206 (1998).

[23] P. Roy, S. Sarkar, J. Alam and B. Sinha, Nucl. Phys. **A 653** 277 (1999).

[24] C. Song, P. W. Xia and C. M. Ko, Phys. Rev. **C52**, 408 (1995).

[25] J. Alam, S. Sarkar, P. Roy, B. Dutta-Roy and B. Sinha, Phys. Rev. **C59**, 905 (1999).

[26] H. A. Weldon, Ann. Phys. **228**, 43 (1993).

[27] J. D. Bjorken, Phys. Rev. **D27**, 140 (1983).

[28] M. Asakawa and T. Hatsuda, Phys. Rev. **D55**, 4488 (1997).

[29] P. Braun-Munzinger, J. Stachel, J. P. Wessels and N. Xu, Phys. Lett. **B 365**, 1 (1996).

[30] A. Dumitru and D. H. Rischke, Phys. Rev. **C59**, 354 (1999).

[31] H. Appelshauser *et.al*, NA49 Collaboration, Eur. Phys. J. **C2**, 661 (1998).

[32] F. Karsch, Nucl. Phys. (proc. suppl.) **B83**, 14 (2000); hep-lat/9909006.

[33] J. Kapusta, P. Lichard and D. Seibert, Phys. Rev. **D 44**, 2774 (1991).

[34] K. Kajantie, M. Kataja, L. McLerran and P. V. Ruuskanen, Phys. Rev. **D34**, 811 (1986).

[35] E. Shuryak, Phys. Rev. Lett. **68**, 3270 (1992).

[36] F. S. Navara, M. C. Nemes, U. Ornik and S. Paiva, Phys. Rev. **C 45**, R2552 (1992).

[37] K. Kajantie, J. Kapusta, L. McLerran and A. Mekjian, Phys. Rev. **D34**, 2746 (1986).

[38] K. Gallmeister, B. Kampfer and O. P. Pavlenko, Phys. Lett. **B 473**, 20 (2000); K. Gallmeister, B. Kampfer, O. P. Pavlenko and C. Gale, hep-ph/0010332.